Q 199606140003

7/33

Effects of Ventilation and Backfill on an Underground Nuclear Waste Repository

R. D. MANTEUFEL
Center for Nuclear Waste Regulatory Analyses
6220 Culebra Road
San Antonio, TX 78238-5166 U.S.A.
(210) 522-5250

submitted to
International Journal of Heat and Mass Transfer

Abstract

The effects of ventilation and backfill on the temperature and relative humidity of waste packages in a mined underground nuclear waste repository are evaluated. The evaluations account for the (i) three-dimensional (3D) transient temperature field created by the heat-dissipating waste out to 10,000 yr, (ii) ventilation of the underground drifts for the first 100 yr, and (iii) emplacement of backfill in the drifts after 100 yr. Three areal mass loading (AML) strategies are evaluated: 20, 40, and 80 MTU/acre. It is found that ventilation removes only a small fraction of the heat yet removes all of the moisture that flows into the drifts. The flow of moisture is minimal for below boiling conditions and is increased greatly for above boiling conditions. Even for the lowest AML of 20 MTU/acre, a dryout zone of 3.3 m radius surrounding the drifts develops and for the highest thermal loading of 80 MTU/acre as much as 8.6 m is dried. The emplacement of low conductivity backfill significantly increases waste packages temperature by over 100°C and leads to low relative humidity to 10,000 yr.

Nomenclature

d_p	mean particle size for backfill [=0.01 m]
D_v	vapor diffusion coefficient in air [$=26\times10^{-6}$ m^2 s^{-1} at 298 K]
D_{wp}	waste package diameter [=1.8 m]
D_d	emplacement drift diameter [=5 m]
g	gravitational constant [=9.81 m s^{-2}]
k	thermal conductivity [W m^{-1} K^{-1}]

L_{rep} total length of ventilated drifts in repository [m]

$\dot{m}_a$ flow rate of dry air [kg s^{-1}]

$\dot{m}''_v$ flux of vapor at the drift wall [kg m^{-2} s^{-1}]

M_a molecular weight of air [=28.97 kg $kmol^{-1}$]

M_v molecular weight of water vapor [=18.02 kg $kmol^{-1}$]

P_v saturated vapor pressure [N m^{-2}]

P_t total gas pressure [= 90,500 N m^{-2}]

Pr Prandtl number [-]

r radial dryout depth [m]

R ideal gas law constant [=8314 J $kmol^{-1}$ K^{-1}]

S_i initial saturation of the host rock [-]

T temperature [K]

U overall vapor transfer coefficient [kg m^{-2} s^{-1})]

GREEK SYMBOLS

α thermal diffusivity [m^2 s^{-1}]

β volumetric thermal expansion coefficient [K^{-1}]

ε thermal emissivity [-]

ν kinematic viscosity [m^2 s^{-1}]

η advective enhancement factor [-]

ϕ porosity [-]

ϕ_{wp} relative humidity at waste package surface [-]

ρ mass density [kg m^{-3}]

σ Stefan-Bolztmann constant [5.67×10^{-8} W m^{-2} K^{-4})]

τ tortuosity [-]

ω humidity ratio [kg water vapor/ kg dry air]

ψ sphericity of particles [-]

SUBSCRIPTS

a dry air

avg average

b boiling point

conv convective

d drift

eff effective

liq liquid water

m intact rock matrix

rad radiative
rep repository
v water vapor
w drift wall
wp waste package

Introduction

There are many challenges associated with the safe, long term geologic disposal of nuclear high-level waste (HLW). One challenge is predicting the integrity of waste packages buried deep in the earth (typically hundreds of meters below the ground surface). In the United States a proposed site is currently being studied at Yucca Mountain (YM), Nevada, which is located at the border of the Nevada Test Site. The site was selected for a number of reasons including the arid nature of the region [1,2]. The current conceptual design consists of tunneling beneath YM and placing the waste in a series of mined drifts. The waste is to be placed in large, thick metal packages designed to safely contain the waste for hundreds and potentially thousands of years [3]. One of the most important aspects affecting waste package lifetime is thermohydrologic environment. Simply stated, waste packages corrode more rapidly if water is present and essentially do not corrode if water is absent. Hence it is important to quantify the environment of heat dissipating waste packages in a mined underground facility.

The thermohydrologic environment of waste packages is affected by a number of conditions: age and thermal output of the waste, spatial arrangement and density of waste packages, thermal and hydraulic properties of the geologic material, ventilation conditions of the mined facility, and possible emplacement of backfill material prior to permanent closure. In the United States high-level radioactive waste program, the current design calls for an extended time period to monitor the waste after emplacement and prior to permanent closure of the repository. During this time, the underground facility will most likely be ventilated for periodic observation and maintenance activities and possibly partial retrieval of waste if needed. It has been recognized that ventilation has a capacity to remove a portion of the waste heat as well as moisture from the underground facility. Heat from the decaying radioactive waste will warm the ventilation air, nearby rock mass, and volatize *in situ* groundwater as well as seeping groundwater that may flow

into a repository drift. The removal of heat and moisture may have significant benefits by developing drier conditions for waste packages after permanent closure.

In many studies of the themohydrologic environment, the effects of ventilation are ignored so that neither heat nor moisture is removed from the subsurface facility [4, 5, 6, 7]. It has been recognized that ventilation has the potential to remove significant amounts of heat and groundwater [1, 8–10]. Only a few studies have evaluated the effects of ventilation on repository mine conditions which are discussed next.

Hopkins et al. [8] describe one- and two-dimensional numerical studies of isothermal moisture removal where liquid was assumed to advect in the rock matrix towards the drift wall and then be removed by ventilation air. Because their model was isothermal, vapor diffusion was neglected as well as the effects of temperature on vapor density and vaporization. Their work then does not represent mine conditions after emplacement of heat dissipating waste.

Danko and Mousset-Jones [9, 10] report numerical predictions of heat and moisture transport in ventilated drifts with heat dissipating waste. Moisture removal is based on a wall wetness ratio discussed in the mine ventilation literature [11, 12]. They conclude that relatively low values of airflow result in large amounts of groundwater removal. Their calculations show "there is a potential that a total amount of 0.72 metric tons of water per linear meter of drift per year can be permanently removed from the repository horizon." They note, however, that the reported potential for water removal may not be consistent with the availability of water to migrate towards the drift. The wall wetness ratio assumes water is readily available at the drift wall. They suggest the wall wetness ratio be adjusted using a coupled hydrothermal model.

Manteufel [13] describes a diffusion controlled drying model for a fractured porous medium. The groundwater is assumed to be essentially stationary. The heat dissipating waste increases the temperature of the host rock and thus the vapor pressure of the groundwater which then motivates vapor diffusion to the relatively dry drift. The model was applied to the low-permeability, fractured rock present at YM. The model was found to be acceptably accurate when compared to a more detailed computer code. However, the model was one-dimensional and did not account for the removal of heat by ventilation.

Ramirez [14] observes that drying of the geologic material will be enhanced if pressure driven gas flow occurs due to temperatures exceeding the boiling point. This was found in field experiments where the elevated temperatures motivated vapor flow from the low permeability rock matrix into fractures which have much lower resistance to flow. The fractures act as preferential flow paths for gas flow. If the temperature, however, remains below the boiling point, then gas flow will be less significant in enhancing dryout. In addition, during drying and imbibition experiments, small fractures have been observed to inhibit liquid transport in the media [15].

Buscheck and Nitao [6] describe a design strategy for the repository where heat dissipating waste is placed relatively close together to elevate subsurface temperatures above the boiling point and drive the groundwater away from the waste. A large dryout zone is created around the waste and potentially hundreds to thousands of years are required for the groundwater to return to the waste packages. In this and other studies, it was found that a dryout zone is created around the waste. The groundwater driven from this zone condenses and collects in a band outside the boiling point isotherm. The potential deleterious effects of this wet zone have been recognized such as focused drainage along fractures and onto cooler waste packages. A significant potential benefit of ventilation during the first 100 yr is that the vaporized groundwater is removed from the system. It does not collect and potentially drains into unfavorable locations.

Repository Layout

In Figure 1, a conceptual design is shown for the proposed repository at YM, Nevada. The design process is ongoing and a final design has not been established [3]. The repository is expected to have two large sloping access ramps (7.62 m diameter), two large vertical ventilation exhaust shafts (~4 m diameter), and a series of horizontal emplacement drifts (~5 m diameter). The waste emplacement drifts will be located off main access drifts connected to the access ramps. The size of the repository remains a design option, as well as the spacing between emplacement drifts and the spacing of waste packages inside each drift. Many conceptual designs have a drift diameter of 5 m and drift spacing from 25 to 50 m [3, 16].

Figure 2 presents a conceptual design for a waste package [3]. In this design, waste packages are introduced into the repository on a rail system using emplacement carts. The

7/33

emplacement carts may be left in the facility or the packages transferred onto holding beds. Leaving the packages on the carts helps to minimize handling of the packages and may facilitate retrieval of waste if necessary.

The monitoring and operational time period of the repository may extend as long as 150 yr [3] during which the region between the waste package and the drift wall probably will not be backfilled. This allows for retrievability of the waste should unfavorable conditions develop in the facility. During this time, either continuous or periodic ventilation will be used to cool areas of the repository and provide oxygen for personnel. The emplacement drifts could be sealed using doors or some ventilation may be permitted through emplacement drifts.

Thermal Loading Strategy

In the design of a repository, attention is often focused on factors that affect the temperature and humidity conditions of the waste packages. These include the (i) spatial density of waste which is measured by the AML of the repository, (ii) age of waste at time of emplacement, (iii) payload of individual waste packages, (iv) ventilation during the operation time period, and (v) time of backfill. This paper focuses on the effects of ventilation and backfill for three AMLs. AML is measured by the MTU of waste per area of repository footprint (traditionally measured in acres). For a fixed waste package payload, the areal mass loading is controlled by drift and package spacing. The AMLs considered are 20, 40, and 80 MTU/acre which represent the range frequently considered [3]. For this analysis the drift spacing is either 60, 35, or 25 m and the waste package spacing is either 30, 25, or 18 m for the 20, 40, or 80 MTU/acre case, respectively. These cases represent a spectrum of strategies including spreading the waste so there is minimal thermal effect created by the repository (20 MTU/acre) or concentrating the waste to enhance thermal effect (80 MTU/acre).

The age of the waste and the size of the waste package are not varied in this analysis. The heat dissipated by the waste is calculated assuming a hypothetical average waste package. The package is an average of a 21 assembly pressurized water reactor (PWR) spent fuel package and a 40 assembly boiling water reactor (BWR) spent fuel package. The average PWR assembly contains 0.45 metric tons of Uranium (MTU) and has a burnup of 42 GWd/MTU. The average

BWR assembly contains 0.19 MTU and has a burnup of 32 GWd/MTU. About 35 percent of the spent fuel requiring disposal is expected to be BWR and 65 percent PWR. This results in an average package containing 8.8 MTU with an average burnup of 38.5 GWd/MTU. The average age of the waste is 26 yr from reactor at the time of emplacement. The thermal output of the waste is calculated using results from ORIGEN2 [Appendix 1C of Ref. 17]. Representative values of the thermal output are shown in Table 1.

Figure 3 provides a conceptual ventilation strategy. Here, fresh ventilation air enters the facility through the sloping inlet ramp and exits through a vertical exhaust shaft. If ventilation of the emplacement drifts is desired, the inlet flow will probably be split into a number of branches. The total length of emplacement drifts to be ventilated depends on the AML strategy and the total repository payload. The repository is currently designed for 70,000 MTU of which 63,000 MTU will be spent fuel. A total of 7,160 spent fuel packages having an average payload of 8.8 MTU will be required to accommodate this waste. About 215 km of emplacement drifts are required for the 20 MTU/acre strategy, 180 km for 40 MTU/acre, and 129 km for 80 MTU/acre. A feasible ventilation strategy will be to split the inlet air into a manageable number of branches (10 to 20) which then ventilate a number of emplacement drifts (7 to 15) in series before exiting the facility. The emplacement drifts are about 1.2 km long [3]. In this way, a sufficient flowrate is achieved in each drift to maintain well-mixed turbulent conditions and avoid stagnant zones.

Drift-Scale Model

A drift-scale model is used to simulate the transient temperature field surrounding a single waste package in the interior of the repository. The drift-scale model extends from the ground surface to deep into the saturated zone below the repository. The ground surface is located 350 m above the repository and the lower boundary is 1000 m below the repository which is 750 m below the water table. Six distinct thermal-geologic units are included in the model and their properties are summarized in Table 2. These values are representative of average conditions and are consistent with those used in other studies [18–21].

In Figure 4, the finite element mesh for the 40 MTU/acre strategies is shown. Only the elements immediately surrounding the waste package are shown with many more elements

extending both above and below. The four vertical sides of the model represent symmetry (therefore adiabatic) conditions. Along the drift, a symmetry condition exists both at the middle of a waste package and at the middle between waste packages. Hence the width of the model along the drift axis is one-half the waste package spacing within a drift (third axis in the model). Similarly, the mid-plane between drifts and a vertical plane through the centerline of a drift represent symmetry conditions. The width of the model (first axis in the model) is one-half the spacing between drifts. The computational model contains only one-quarter of a waste package. Each model consists of 5,210 nodes and 2,960 elements. A commercially available program ABAQUS [22] is used to solve the transient heat transfer problem.

Four distinct regions exist in each model: host rock, waste package, floor (shaded elements), and backfill. The backfill elements are not shown in Figure 4 but do exist in the mesh. Floor conductivity is based on published estimates [19, 20]. The waste package has a high thermal conductivity and is essentially isothermal. The effective thermal conductivity of the region between the waste package and the drift wall is changed at the time of backfilling and is discussed next.

Backfill Conductivity Models

A temperature dependent thermal conductivity model was developed for the backfill region for both the unbackfilled case (air only) and the backfilled case (crushed rock). The effective thermal conductivity is based on a linear combination of conductive/convective and radiative models. Prior to backfilling, the conductivity is relatively high due to buoyant natural convection and radiative transfer from the waste package surface to the drift wall. After backfilling, the conductivity is relatively low because of the insulating effects of the crushed rock which eliminates buoyant gas flow and reduces the effectiveness of thermal radiation.

An effective conductivity model for natural convection in a cylindrical enclosure with a concentric cylindrical heat source is used to estimate radiative transfer from the cask to the drift wall [23].

$$k_{conv} = 0.386\ k_a \left(\frac{Pr}{0.861 + Pr}\right)^{1/4} \left[\frac{\left[\ln\left(D_d / D_{wp}\right)\right]^4 g\ \beta\ \Delta T}{\nu\ \alpha\ \left(D_{wp}^{-3/5} + D_d^{-3/5}\right)^5}\right]^{1/4} \tag{1}$$

where the drift diameter is $D_d = 5$ m, the waste package diameter is $D_{wp} = 1.8$ m, the Prandtl number for air is Pr = 0.7, and the ratio $(g\ \beta)/(\nu\ \alpha)$ for air at 100°C is about 36×10^6 m^{-3} K^{-1}. The ΔT from the waste package to the drift wall is assumed to be about 20°C. Because the floor blocks some of the flow, the actual convective heat transfer will be less than predicted assuming no floor (i.e., a suspended waste package). It is presumed that convection would be reduced by one-half due to the floor. As a result, the convective contribution using equation (1) is estimated to be 30 times the air conductivity

$$k_{conv} = 30\ k_a \tag{2}$$

The effective radiative conductivity is derived by equating the conductive transfer through an effective conductivity medium and the radiative transfer from the waste package surface to the surrounding drift wall, which yields

$$k_{rad,nobackfill} = \varepsilon\ \frac{D_{wp}}{2}\ \sigma\ 4\ T^3\ \ln\left(\frac{D_d}{D_{wp}}\right) \tag{3}$$

where the emissivity of the waste package is assumed to be $\varepsilon = 0.8$. The overall effective conductivity is the sum of radiative and convective contributions, $k_{eff} = k_{rad,nobackfill} + k_{conv}$, and is shown in Table 4 for a range of temperatures. In the unbackfilled drift, heat transfer is dominated by radiation. At 200°C the conductivity is 20 W m^{-1} K^{-1} which is consistent with other work [19]. For practical purposes, the natural convection contribution is negligible so that the precision of equation (1) is not of overall importance.

During backfilling, the waste package is expected to be covered with a crushed rock, probably the same type as originally extracted during excavation. The air is assumed to be essentially stagnant in this media, and the mean free path for radiative transfer is expected to be small. An effective conductivity is sought with contributions from conduction and radiation through the media.

A number of relations have been developed for the effective conductivity of an unconsolidated media. Five models were reviewed to gauge the range of anticipated backfill conductivity [24–28]. The models are summarized in the Appendix.

In Figure 5, the conductivity models are compared assuming rock excavated from the repository horizon at YM is used as backfill material. The rock has an intact conductivity of 2.1 W m^{-1} K^{-1} and air is about 0.026 W m^{-1} K^{-1} at 300 K. The porosity of the crushed backfill is uncertain and is estimated to range from 40 to 60 percent. Considering the variation between models and the uncertainty in backfill porosity, conductivity is estimated to range from 0.1 to 0.5 W m^{-1} K^{-1}. For this problem, a value of 0.20 W m^{-1} K^{-1} is adopted and combine with the radiative conductivity.

A radiative conductivity is based on a mean pore size which limits radiative transfer. A number of radiative conductivity models have been developed for packed particle beds. All of the models depend strongly on the mean pore size which for this problem is uncertain (or possibly can be considered a design controlled parameter). A simple and robust model that has been applied to a number of problems [30, 31] is adopted here

$$k_{rad,backfill} = \varepsilon \; d_p \; \sigma \; 4 \; T^3 \qquad (4)$$

where the mean particle size is assumed to be about $d_p = 1$ cm and the emissivity of the rock is estimated to be about ε=0.8. The combined effective conductivity for the backfill is evaluated and presented in Table 3. Other analyses assume constant values of 0.4 W m^{-1} K^{-1} and 0.6 W m^{-1} K^{-1} [20], which are consistent with Table 3 in the range of 200 to 350°C. Recent experimental measurements reporte values in the range of 0.58 to 0.74 W m^{-1} K^{-1} [32], however, these results are based on larger particle sized (1.2 to 3.8 cm) which accentuated radiative transfer. Overall, the values in Table 3 are consistent with available data.

Moisture Removal Model

One of the challenges in modeling subsurface moisture removal is that the host rock at YM is fractured and of relatively low matrix permeability (about two microdarcy) [21]. Hence, liquid is not necessarily advected to the drift walls where it can vaporize. The fractures and low

permeability matrix encourages vaporization of groundwater where it originally resides in the rock. The vapor will then flow by either diffusion (due to a vapor density gradient) or advection (due to total gas pressure gradient). The dominant vapor transport mechanism is related to the temperature. If the temperatures remain below the boiling point, diffusive transport will dominate. If temperatures exceed the boiling point, then pressure driven flow dominates and dryout will be significantly enhanced.

Removal of moisture by ventilation is distinctly different than heat removal. Because of the low specific heat of air and the relatively large convective heat transfer coefficient between the air and the drift wall and between the air and the waste package surface, the air will warm within a short distance in the drifts. As a result, the sensible heating of the air is accomplished by a relatively small fraction of the waste packages in the repository, that is, those located where ventilation is first introduced into the repository. For this work, it is assumed the ventilation flow pattern is periodically changed so that all waste packages contribute uniformly to the sensible heating of the air. A result of this assumption is that the average waste package temperature will be slightly underestimated as well as the extent of rock dryout.

In contrast, not enough moisture is available to saturate the ventilation air. Moisture pickup is limited by the transport of moisture from the rock into the drift. With ventilation, the air remains relatively dry and the humidity ratio, ω, increases steadily along the drift. A diffusion controlled model is used to predict the extent and rate of rock dryout. Because of the low matrix permeability, dryout is modeled as if a vaporization front penetrates into the media [13]. The flow of vapor from this front into the drift is predicted using Fick's law.

$$\dot{m}''_v = U\left[x_v(r) - x_v(0)\right] \tag{5}$$

where r is the depth of dryout measured from the drift wall, and $x_v(r)$ and $x_v(0)$ are the vapor mass fractions at the vaporization front and drift wall, respectively [23]. The overall vapor transfer coefficient (related to the reciprical of resistance) is defined for this problem to be:

$$U = \frac{\eta\ \bar{\rho}\ \tau\ \phi\ D_v}{\frac{D_d}{2}\ \ln\left(\frac{2r + D_d}{D_d}\right)} \tag{6}$$

where the advective enhancement factor is η, the average density of the humid air is $\bar{\rho}$, the tortuosity in the media is assumed to be $\tau \cong 0.67$ [33], the porosity in the media is approximately ϕ=0.1 [18], the molecular diffusion coefficient of vapor in air is D_v, and the drift diameter is $D_d = 5$ m. The advective enhancement factor accounts for gas flow induced by the diffusion of water vapor, especially as the temperature approaches the boiling point

$$\eta = \frac{P_t}{P_t - P_v} \tag{7}$$

where the total gas pressure at YM is about $P_t = 90.5$ kPa corresponding to a boiling point temperature of $T_b = 97°C$. The vapor pressure is calculated at the temperature of the vaporization front. The advective enhancement factor is doubled for every degree above 96°C to provide a smooth transition from equation (7) and simulate above boiling conditions. In this way, the vaporization front will approximately follow the boiling point isotherm if it expands faster than the dryout zone (typically for high AML cases). The average mass density of the air-vapor mixture is

$$\bar{\rho} = \rho_a + \rho_v \tag{8}$$

The air and vapor densities are calculated using the ideal gas law and the assumption that the vapor is in equilibrium with the liquid at the vaporization front. The vapor pressure at the vaporization front equals the saturated vapor pressure which depends on the temperature of the front. If the vaporization front temperature exceeds the boiling point, the vapor pressure is limited to the total pressure and the air pressure equals zero. In general the air partial pressure is $P_a = P_t - P_v$. The air density then is $\rho_a = P_a M_a/(RT)$ and similarly the vapor density is $\rho_v = P_v M_v/(RT)$. The vapor diffusion coefficient is scaled with respect to temperature [34] from a datum point of $D_o = 26 \times 10^{-6}\ m^2\ s^{-1}$ at $T_o = 298$ K.

$$D_v = D_o \left(\frac{T}{T_o}\right)^{3/2} \tag{9}$$

The mass fraction of vapor at the vaporization front is

$$x_v(r) = \begin{cases} 1 & \text{if } T(r) \geq T_{boil} \\ \dfrac{\rho_v}{\rho_a + \rho_v} & \text{otherwise} \end{cases} \tag{10}$$

The mass fraction of vapor in the ventilated drift can be calculated considering conservation of water for the ventilated drift

$$\dot{m}_a(\omega_e - \omega_i) = U\left(\pi D_d L_{rep}\right)\left[x_v(r) - x_v(0)\right] \tag{11}$$

where the ventilation flowrate of dry air is $\dot{m}_a$, and the inlet and exit humidity ratios are ω_e and ω_i, and the total drift length of the repository is L_{rep} which depends on the AML. The humidity ratio (or absolute humidity) is defined as the ratio of mass of vapor per mass of dry air, $\omega = \rho_v / \rho_a$. In comparison, the vapor mass fraction in the drift is $x_v(0) = \rho_v / (\rho_a + \rho_v)$. With ventilation, the drift vapor density remains low so that $\rho_a >> \rho_v$ and the average vapor mass fraction equals the average humidity ratio in the drift, $x_v(0) = \omega_{avg} = (\omega_i + \omega_e)/2$. Based on the conservation of vapor in the system, an expression for the average vapor mass fraction in the drift can be derived

$$x_v(0) = \frac{2\ \dot{m}_a\omega_i + U\left(\pi D_d L_{rep}\right)x_v(r)}{2\ \dot{m}_a + U\left(\pi D_d L_{rep}\right)} \tag{12}$$

High ventilation flowrates drive the average drift humidity ratio to that of the inlet humidity ratio. If the ventilation flowrate is zero, the drift vapor mass fraction equals the vapor mass fraction at the dryout front.

Based on hourly readings over the past 17 yr from the National Weather Service station at Desert Rock, Nevada [29], the humidity ratio of surface air is estimated to range from 0.0025 to 0.0065 with a yearly average of ω_i=0.0038.

The extent of the dryout zone is calculated by integrating the rate of water removed, thus tracking the location of the dryout front

$$\frac{dr}{dt} = \frac{U\left[x_v(r) - x_v(0)\right]}{\phi\ S_i\ \rho_{liq}\left(\dfrac{2r}{D_d} + 1\right)} \tag{13}$$

where the initial groundwater saturation in the host rock is about S_i =0.8 and the matrix porosity is about ϕ=0.1 [21]. The initial dryout depth is nearly zero, r = 0.001 m, to avoid a singularity in equation (13).

Removal of groundwater depends on the ventilation mass flow rate. Current conceptual designs of the repository call for a sustainable air flow rate of 125 kg s^{-1} in both the emplacement side and the operation side of the repository [3]. A maximum design flow rate of 580 kg s^{-1} is also possible if retrieval of waste is to be undertaken. For this work, a reasonable continuous flow rate of 125 kg s^{-1} is assumed for the entire repository for the first 100 yr.

To conserve energy, latent heat associated with volatizing groundwater and sensible heat associated with warming the ventilation air is subtracted from the waste package heat source. This energy, as well as the associated groundwater, is permanently removed from the subsurface facility by the ventilation.

The relative humidity at the waste package surface is considered important in predicting the corrosion and subsequent failure of waste packages. Because the waste package temperature is frequently higher than T_b and the total pressure is approximately constant for an unsaturated repository, the relative humidity is defined as the ratio of actual vapor pressure to saturated vapor pressure at T_{wp}. While the facility is ventilated, the relative humidity at the waste package surface is given by

$$\phi_{wp} = \frac{M_a \ \omega_{avg} \ P_t}{M_v \ P_v(T_{wp})} \tag{14}$$

After ventilation stops, the vapor mass fraction at the waste package equals that at the vaporization front where liquid water is available. The dryout front is assumed to retreat with the boiling point isotherm. When the boiling point isotherm returns to the drift wall, the wall temperature is used to calculate the vapor mass fraction. Without ventilation, the relative humidity then is given by

$$\phi_{wp} = \frac{P_v(\min(T_b, \ T_w))}{P_v(T_{wp})} \tag{15}$$

The extent of heat and moisture removal is discussed in the results section.

Results

In Figure 6, vertical temperature profiles are plotted at six different times for the 40 MTU/acre case. The profiles are taken along the edge of the 3D model going through the center of the waste package. After 100 yr, the thermal perturbation generated by the waste propagates about 100 m above and below the repository. Hence, accurate calculations of waste package conditions require accurate predictions of far-field conditions. The waste package temperatures appear are much higher than the host rock temperatures 5 m into the rock. This is due to the low conductivity of the backfill and floor. The waste package is effectively isothermal. Prior to backfilling, the space above the package has a high conductivity so that isotherm is somewhat distorted and the drift wall above the package is hotter than that below. After backfilling, the conductivity is much lower and the temperature gradient is much higher. Here, the top of the drift wall is cooler than the bottom.

In Figure 7, the waste package temperature, average drift wall temperature, and relative humidity at the waste package are shown for 20, 40, and 80 MTU/acre AMLs. It can be observed that the AML strategy has a strong effect on the waste package and drift wall temperatures. Prior to backfilling, the waste package temperature peaks at 120°C at 8 yr for 20 MTU/acre, 125°C at 15 yr for 40 MTU/acre, and 160°C at 50 yr for 80 MTU/acre. For the lowest AML, the drift wall temperature remains below the boiling point for all times. For the highest AML, the drift wall temperature exceeds the boiling point temperature from about 10 yr to about 3,000 yr. As a result, the groundwater is more readily vaporized for the higher AML leading to greater dryout. Without ventilation, relative humidity at the waste package is similar for both the 20 and 40 MTU/acre cases but is lower for the 80 MTU/acre case. The higher AML drives the waste package temperature higher so relative humidity decreases.

Both ventilation and backfill have strong effects for all cases. Ventilation readily maintains dry conditions in the drifts. For the lowest AML, ventilation has a minimal influence on temperatures. For the highest thermal load, however, ventilation has a stronger affect. For the 80 MTU/acre case, the waste package temperature is over 30°C lower (120°C instead of 155°C) with

ventilation. Similarly, ventilation noticeably lowers the drift wall temperature by about 30°C for the 80 MTU/acre case. Backfill always has the pronounced result of increasing the waste package temperature by about 100°C. After time, however, the thermal output of the package decreases and the package temperature is within 10°C of the drift wall temperature within a few thousand years. Backfill has a strong long-lasting affect on relative humidity for all thermal loads to 10,000 yr. Promptly after backfill, the relative humidity is about 5 percent for all AMLs. The rate of increase in humidity is about the same for the 20 and 40 MTU/acre cases. The 80 MTU/acre case maintains lower relative humidity for a few thousand years and slowly increases to nearly 75 percent at 10,000 yr.

In Figure 8, the extent of dryout is compared for the difference cases. Because the highest AML attains higher temperatures, it drives more moisture from the host rock. About 3.3, 4.8, and 8.6 m of rock are dried for the 20, 40, and 80 MTU/acre cases. The most significant effect of ventilation is not necessarily cooling of the repository, but desiccation of the facility. When ventilation is employed, some groundwater is removed from the system instead of being redistributed in the host rock.

Conclusions

In this work the effects of ventilation and backfill are quantified using three AML strategies. Ventilation and backfill are shown to have significant effects on the relative humidity and temperature in an underground HLW disposal facility. The results show the following.

1. For low AML strategies (20 and 40 MTU/acre), ventilation does not remove a significant amount of heat from the repository. For the highest AML (80 MTU/acre) ventilation removes enough heat to lower the maximum waste package temperature by about 30°C (from 155°C to 125°C).

2. Ventilation is effective at removing moisture from the repository. The extent of dryout is about 3.3 m for 20 MTU/acre, 4.8 m for 40 MTU/acre, and 8.6 m for 80 MTU/acre case.

3. In many previous hydrothermal analyses, the repository heat leads to condensate buildup in cooler locations. This buildup has the potential to drain onto cooler waste packages. By

ventilating the repository, uncertainties associated with condensate buildup and refluxing are diminished.

4. Backfilling the emplacement drifts with crushed, unconsolidated tuff has a significant and persistent effect on the temperature and relative humidity of waste packages. Promptly after backfilling at 100 yr, the waste package temperatures increase by about 100°C over unbackfilled temperatures (from 75 to 175°C for 20 MTU/acre, from 100 to 200°C for 40 MTU/acre, and from 120 to 225°C for 80 MTU/acre). Relative humidity remains low for hundreds to thousands of years. Without backfill, the relative humidity reaches 75 percent within a few hundred years, yet with backfill over 10,000 yr are required before the relative humidity reaches 75 percent.

These analyses suggest that ventilation and backfill can be used to create desirable thermohydrologic conditions for waste packages and these conditions may persist for hundreds to thousands of years. Ventilation has the most promising advantage of alleviating uncertainties about groundwater condensate buildup and possible refluxing.

Acknowledgments

This paper was prepared to document work performed by the Center for Nuclear Waste Regulatory Analyses (CNWRA) for the U.S. Nuclear Waste Regulatory Commission (NRC) under Contract No. NRC-02-93-005. The activities reported herein were performed on behalf of the NRC Office of Nuclear Material Safety and Safeguards (NMSS), Division of Waste Management (DWM). The report is an independent product of the CNWRA and does not necessarily reflect the views or regulatory position of the NRC. Editorial review by B. Long, technical review by A.H. Chowdhury, and programmatic review by B. Sagar helped improve the quality of this paper.

References

1. E.H. Roseboom, Disposal of high-level nuclear waste above the water table in arid regions, Geological Survey Circular 903, U.S. Geological Survey, Alexandria, VA (1983).

2. Site characterization plan: Yucca Mountain site, Nevada research and development area, Nevada, DOE/RW-0199, U.S. Department of Energy, Washington D.C. (1988).

3. Initial summary report for repository/waste package advanced conceptual design, B00000000-0-5705-00015, Rev. 00, TRW Environmental Safety Systems, Las Vegas, NV (1994).

4. K. Pruess, Y.W. Tsang and J.S.Y. Wang, Numerical studies of fluid and heat flow near high-level nuclear waste packages emplaced in partially saturated fractured tuff, LBL-18552, Lawrence Berkeley Laboratory, University of California, Berkeley, CA (1984).

5. K. Pruess, J.S.Y. Wang and Y.W. Tsang, On thermohydrologic conditions near high-level nuclear wastes emplaced in partially saturated fractured tuff 1. Simulation studies with explicit consideration of fracture effects, *Water Resources Res.* **26**(6), 1235–1248 (1990).

6. T.A. Buscheck and J.J. Nitao, Repository-heat-driven hydrothermal flow at Yucca Mountain, Part I: Modeling and analysis, *Nuclear Tech.* **104**, 418–448 (1993).

7. C. Doughty and K. Pruess, A similarity solution for two-phase fluid and heat flow near high-level nuclear waste packages emplaced in porous media, *Int. J. Heat Mass Transfer* **33**(6), 1205–1222 (1990).

8. P.L. Hopkins, R.R. Eaton and S. Sinnock, Effect of drift ventilation on repository hydrology and resulting solute transport implications. In *Flow and Transport Through Unsaturated Fractured Rock,* Geophysical Monograph 42, pp. 177–183. American Geophysical Union, Washington D.C. (1987).

9. G. Danko and P. Mousset-Jones, Coupled heat and moisture transport model for underground climate prediction. In *International High-Level Radioactive Waste Management Conference*, pp. 790–798. American Nuclear Society, La Grange Park, IL (1992).

10. G. Danko and P. Mousset-Jones, Modeling of the ventilation for emplacement drift re-entry and rock drying. In *International High-Level Radioactive Waste Management Conference*, pp. 590–599. American Nuclear Society, La Grange Park, IL (1993).

11. *CLIMSIM Climatic Simulation Program, User's Manual*, Mine Ventilation Services, Lafayette, CA (1986).

12. L.W. Laage, R.E. Greuer and W.H. Pomroy, *MFIRE Mine Fire and Ventilation Simulator, Users Manual*, U.S. Bureau of Mines, Minneapolis, MN (1994).

13. R.D. Manteufel, H.M. Castellaw and S.A. Stothoff, Microslab model for diffusion-controlled drying of a fractured porous medium. In *National Heat Transfer Conference*, HTD-309 Vol. 7, pp. 31–40. ASME, NY (1995).

14. A.L. Ramirez, Prototype engineered barrier system field test (PEBSFT) final report, UCRL-ID-106159, Lawrence Livermore National Laboratory, Livermore, CA (1991).

15. A.J. Russo and D.C. Reda, Drying of an initially saturated fractured volcanic tuff, *J. Fluids Eng.* **111**, 191–196 (1989).

16. FY93 thermal loading systems study final report, B00000000-01717-5705-00013 Rev. 01, TRW Environmental Safety Systems, Las Vegas, NV (1993).

17. Characteristics of spent fuel, high-level wastes which may require long-term isolation, DOE/RW-0184 Vol. 2, U.S. Department of Energy, Washington D.C. (1987).

18. Yucca Mountain project reference information base, YMP/93-02 Rev. 3, U.S. Department of Energy, Las Vegas, NV (1993).

19. Wilson, M.L., J.H. Gauthier, R.W. Barnard, G.E. Barr, H.A. Dockery, E. Dunn, R.R. Eaton, D. C. Guerin, N. Lu, M.J. Martinez, R. Nilson, C.A. Rautman, TH. Robey, B. Ross, E.E. Ryder, A.R. Schenker, S.A. Shannon, L. H. Skinner, W.G. Haley, J.D. Gansemer, L.C. Lewis, A.D. Lamont, I.R. Triay, A. Meijer, and D.E. Morris. Total-system performance assessment for Yucca Mountain—SNL second iteration (TSPA-93), SAND93-2675, Sandia National Laboratory, Albuquerque NM (1994).

20. Total system performance assessment—1995: An evaluation of the potential Yucca Mountain repository, B00000000-01717-2200-00136, Rev. 01, TRW Environmental Safety Systems, Las Vegas, NV (1995).

21. R.R. Peters, E.A. Klavetter, I.J. Hall, S.C. Blair, P.R. Heller and G.W. Gee, Fracture and matrix hydrologic characteristics of tuffaceous materials from Yucca Mountain, Nye County, Nevada, SAND84-1471, Sandia National Laboratory, Albuquerque, NM (1984).

22. *ABAQUS Theory and User Manuals*, Hibbitt, Karlsson & Sorensen, Pawtucket, RI (1995).

23. F.P. Incropera and D.P. DeWitt, *Fundamentals of Heat and Mass Transfer* (3rd edn), p. 563. Wiley, NY (1995).

24. J.C. Maxwell, *A Treatise on Electricity and Magnetism,* Vol. 1 (3rd edn), p. 440. Clarendon Press, Oxford (1904).

25. Z. Hashin and S. Shtrikman, A variational approach to the theory of the effective magnetic permeability of multiphase materials, *J. Appl. Phys.*, **33**(10), 3125–3131 (1962).

26. G.R. Hadley, Thermal conductivity of packed metal powders, *Int. J. Heat Mass Transfer* **29**(6), 909–920 (1986).

27. L.S. Verma, R. Singh and D.R. Chaudhary, Geometry dependent resistor model for predicting effective thermal conductivity of two phase systems, *Int. J. Heat Mass Transfer* **37**(4), 704–714 (1994).

28. K. Litchnecker, The electrical conductivity of periodic and random aggregates, *Physik Z.* **27**, 115 (1926).

29. National Climatic Data Center, WBAN hourly surface observations March 1984 through February 1994, National Oceanic and Atmospheric Administration, Asheville, NC (1995).

30. W. Schotte, Thermal conductivity of packed beds, *J. Am. Inst. Chem. Eng.* **6**(1), 63 (1960).

31. J.S. Botterill, A.G. Salway and Y. Teoman, The effective thermal conductivity of high temperature particulate beds. I–Experimental determination. *Int. J. Heat Mass Transfer* **32**(3), 585–609 (1989).

32. E.E. Ryder, R.E. Finley, J.T. George, C.K. Ho, R.S. Longenbaugh and J.R. Connolly, Bench-scale experimental determination of the thermal diffusivity of crushed tuff, SAND94-2320, Sandia National Laboratory, Albuquerque, NM (1996).

33. T.J. Marshall and J.W. Holmes, *Soil Physics* (2nd edn). p. 296. Cambridge University Press, NY (1988).

34. J.H. Lienhard, *A Heat Transfer Textbook* (2nd edn). p. 531. Prentice-Hall, Englewood Cliffs, NJ.

Appendix

The effective conductivity (without radiative transfer) models are summarized here.

Maxwell [24] shown by Hashin and Shtrikman [25] to be an upper bound for a homogeneous, isotropic, two phase mixture

$$k_{eff} = k_m + \frac{\phi}{\dfrac{1}{k_a - k_m} + \dfrac{1-\phi}{3\,k_m}} \tag{A1}$$

and a lower bound

$$k_{eff} = k_a + \frac{1-\phi}{\dfrac{1}{k_m - k_a} + \dfrac{\phi}{3\,k_a}} \tag{A2}$$

Hadley [26] for granular, unconsolidated, two phase mixture

$$k_{eff} = \frac{\phi\ f\ k_a + (1-\phi\ f)\ k_m}{1-\phi(1-f_o) + \phi(1-f_o)k_m / k_a} \tag{A3}$$

where f=0.8, a value consistent with spherical particles [26] which is consistent with the value of f=0.82 found by Verma et al. [27] to yield the best estimates for granular mixtures.

Verma et al. [27]

$$k_{eff} = \left[k_{pl}^2 + k_{pr}^2\right]^{1/2} \tag{A4}$$

where

$$k_{pl} = \left[\phi k_a + (1-\phi)k_m\right]\cos(\theta)$$

$$k_{pr} = \left[\frac{\phi}{k_a} + \frac{1-\phi}{k_m}\right]^{-1} \sin(\theta)$$

$$\theta = \tan^{-1}\left[B_o\ F\ \phi^2\left(\psi\frac{k_m}{k_a}\right)^{1/2}\right]$$

$$F = \frac{1}{\phi}\left[1 + \frac{0.3219(1-\phi)}{\psi}\right]^2$$

For granular media $B_0=1.15$ [27]. The spericity of solid particles, ψ, is defined as the ratio of surface area of an equivalent sphere having the same volume as that of the average solid particle. For spherical particles $\psi=1$, for cubical particles $\psi=0.8$, for rectangular particles with shape 1:1:2 $\psi=0.3$. For crushed rock ψ is unknown but assumed to be $\psi=0.5$ for this work.

Litchnecker [28] also known as the geometric mean model [19]

$$k_{eff} = k_m \left(\frac{k_a}{k_m} \right)^{\phi} \tag{A5}$$

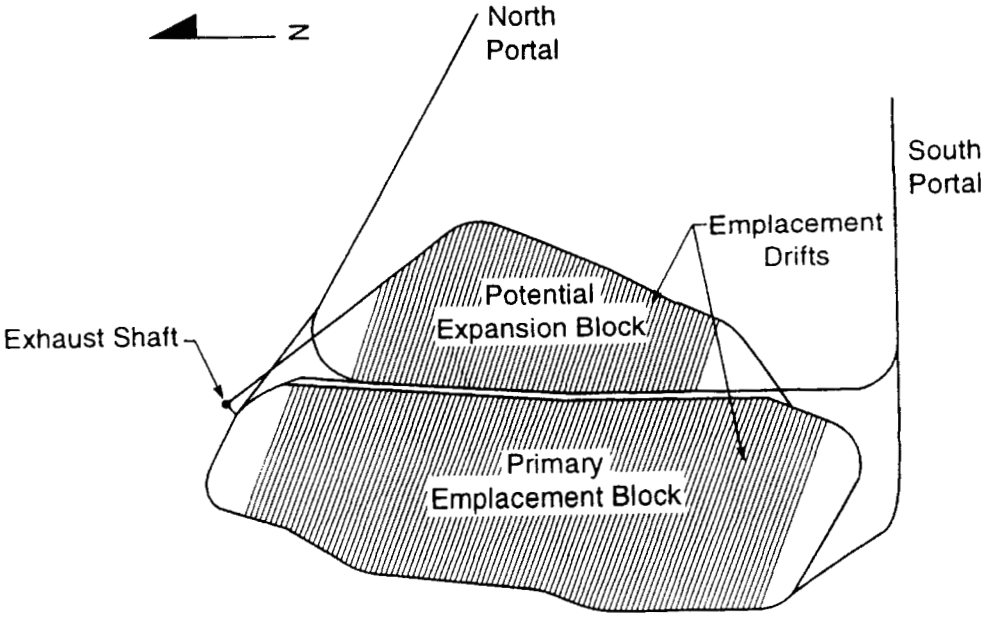

Figure 1. Conceptual repository layout

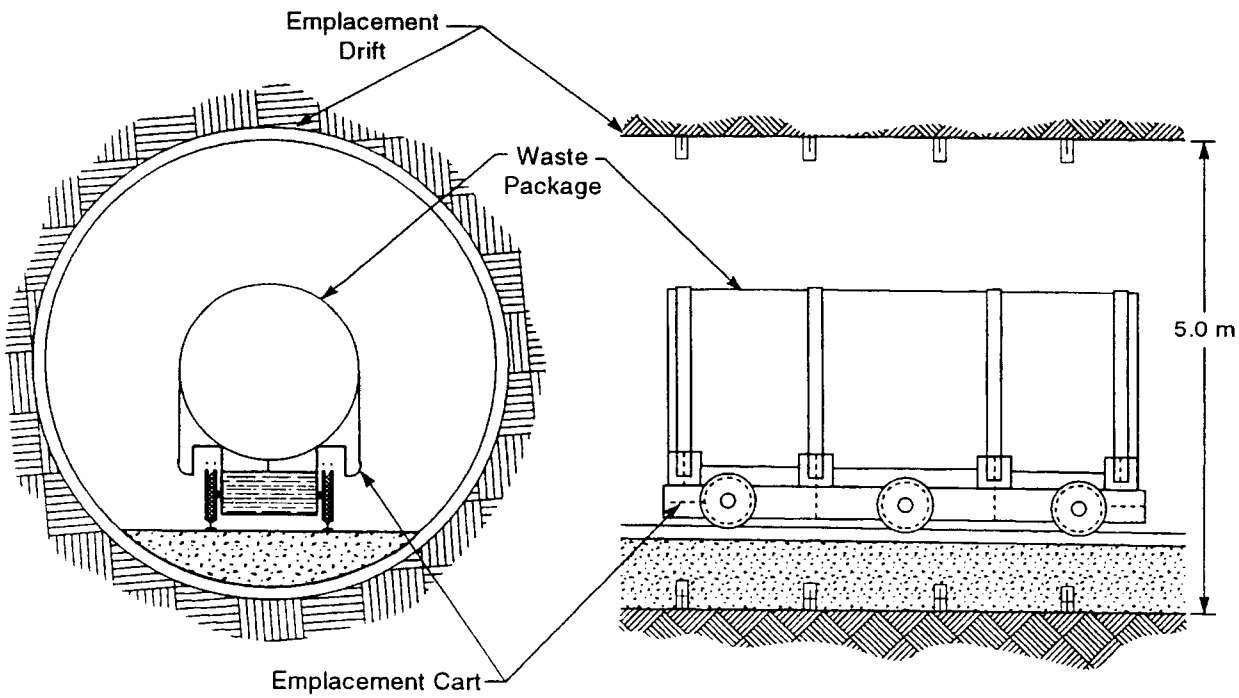

Figure 2. Conceptual in-drift emplacement

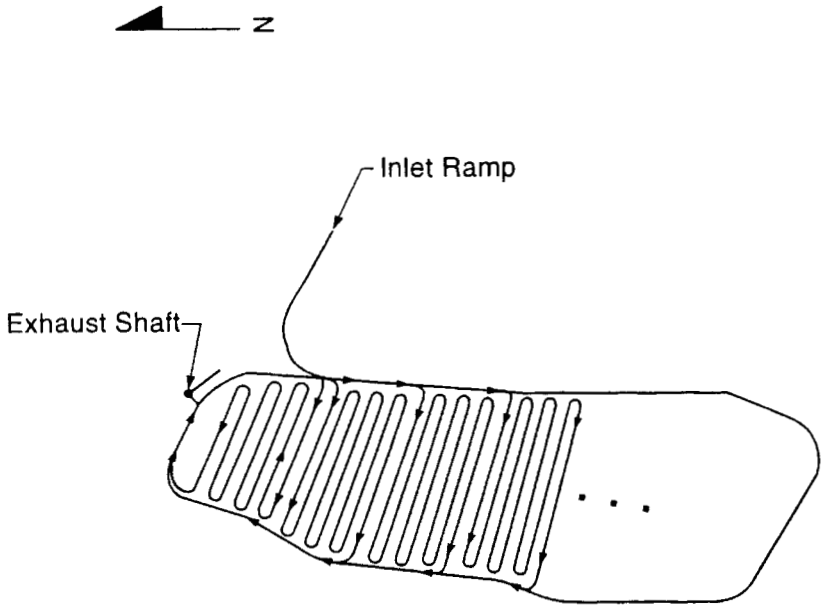

Figure 3. Conceptual ventilation strategy

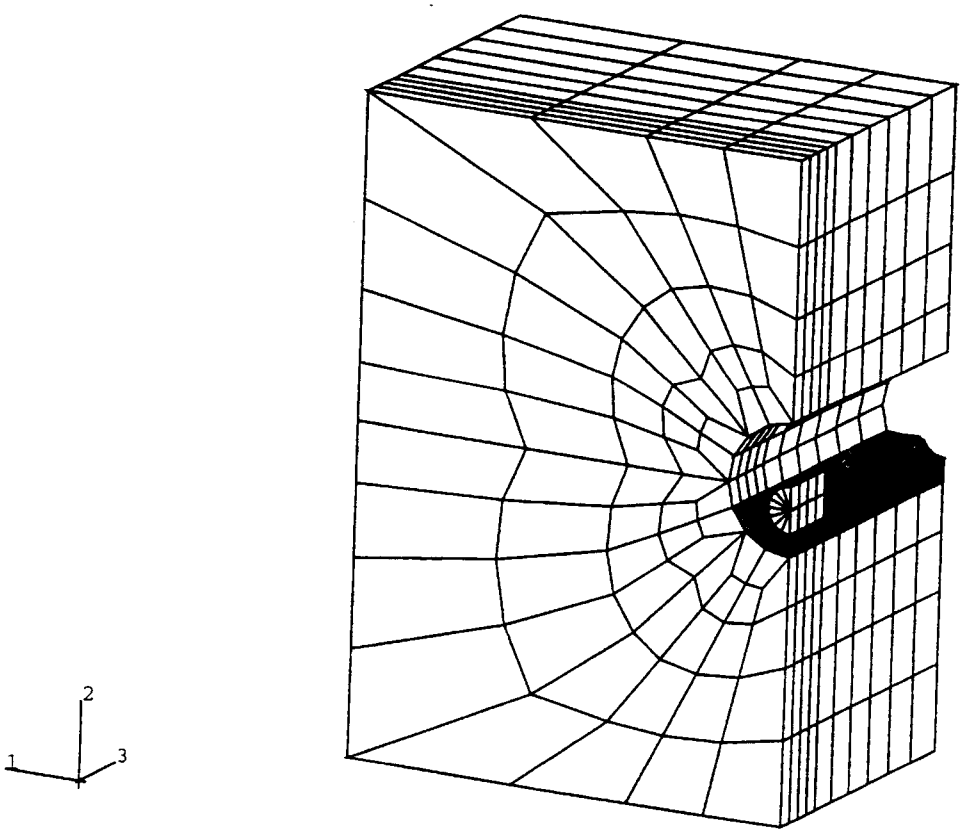

Figure 4. Computational mesh for areal mass loading of 40 MTU/acre. Only elements immediately surrounding the waste are shown for clarity.

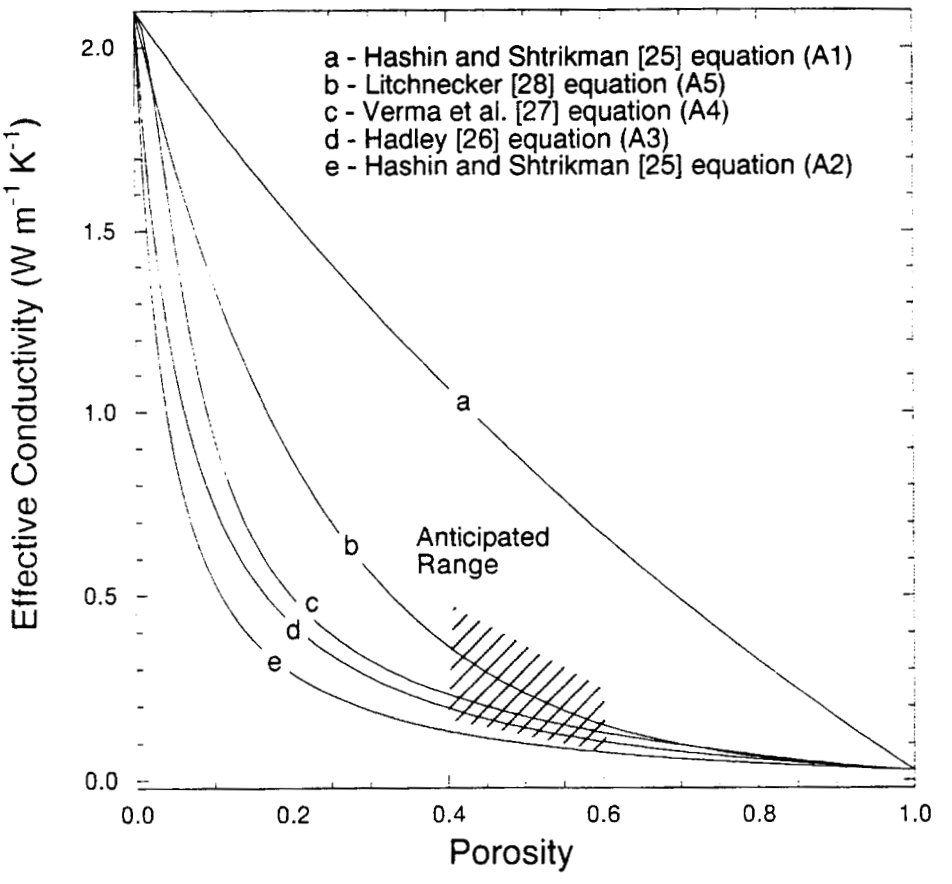

Figure 5. Conduction only conductivity models for unconsolidated backfill

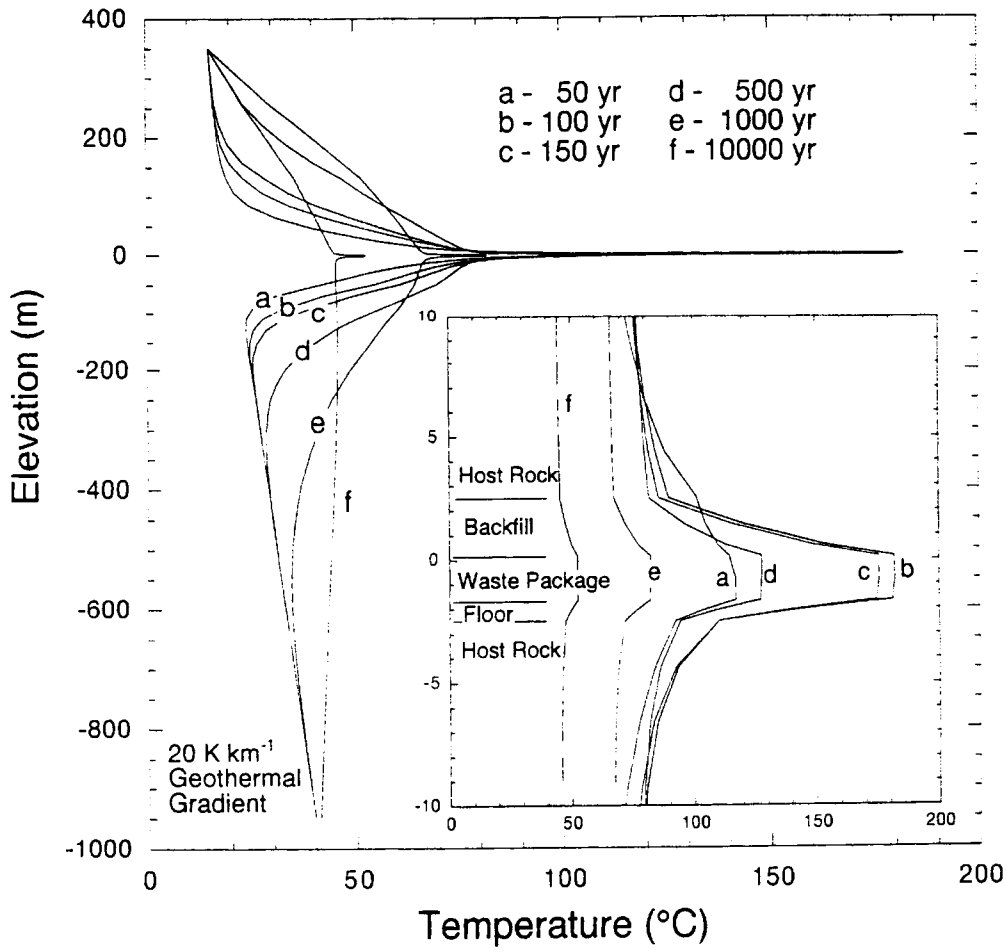

Figure 6. Vertial temperature profile for areal mass loading of 40 MTU/acre

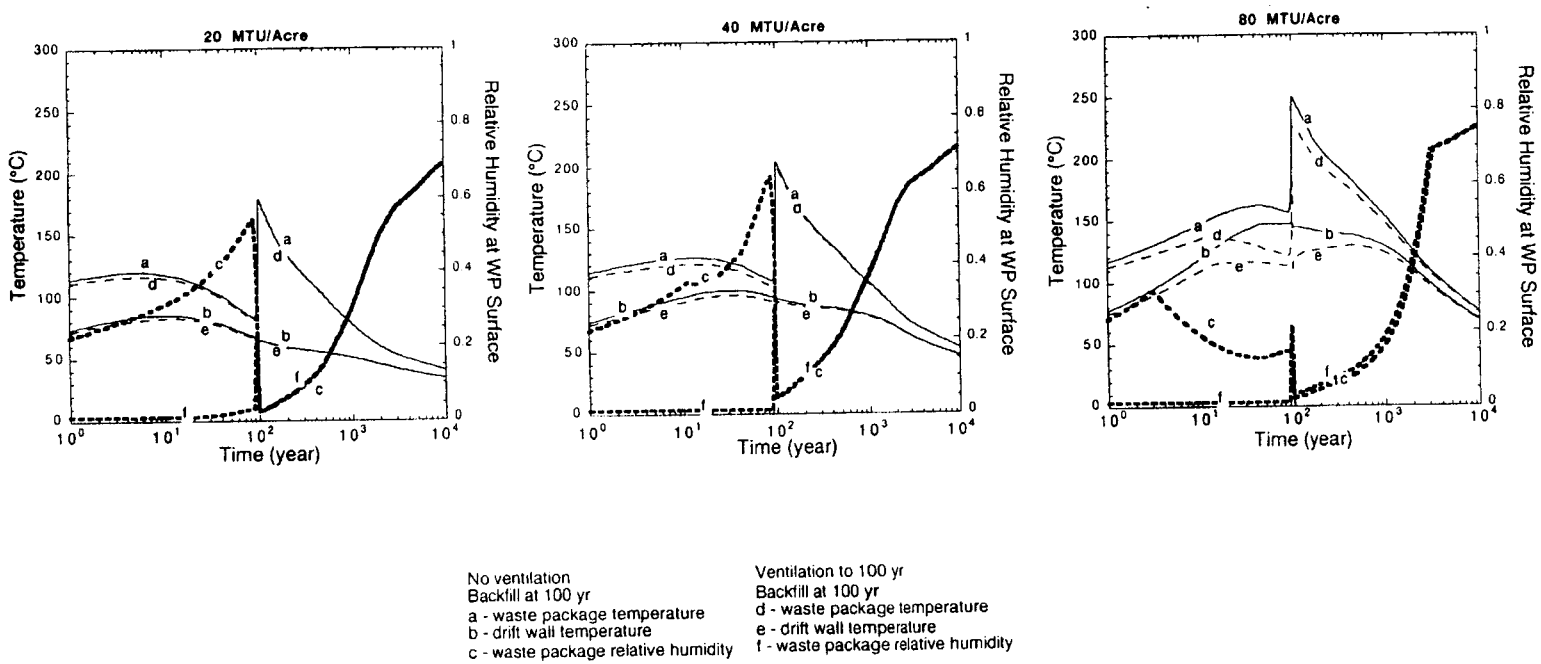

Figure 7. Temperature of waste package and drift wall, and relative humidity at waste package with and without ventilation, and with backfilling at 100 yr. Three areal mass loadings are considered: 20, 40, and 80 MTU/acre.

29/33

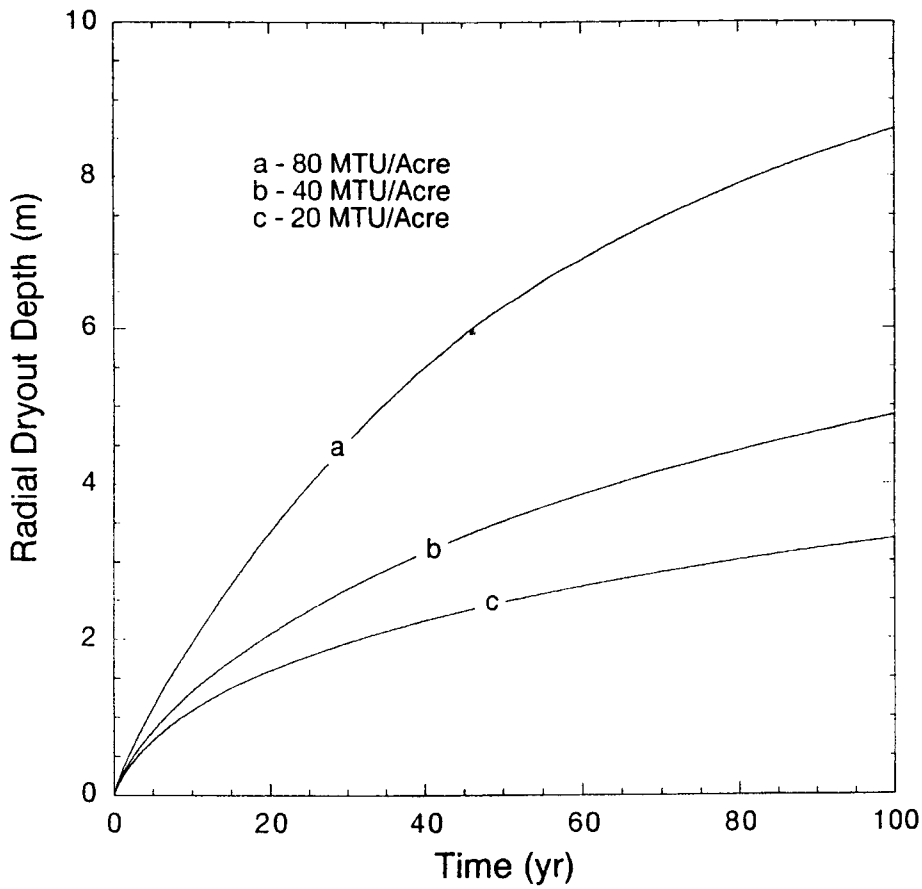

Figure 8. Radial dryout depth

Table 1. Heat Source of Average Spent Fuel Package

Time after emplacement (yr)	Thermal output (W)
0	8016.47
1	7873.61
2	7738.36
5	7346.68
10	6734.76
20	5748.46
50	3841.43
100	2413.61
200	1508.68
500	890.15
1000	516.46
2000	270.60
5000	172.04
10000	124.69

Table 2. Thermal Properties

Thermo-hydrologic Unit	Elevation [m]	Thermal Conductivity [W m^{-1} K^{-1}]	Density [kg m^{-3}]	Specific Heat [J kg^{-1} K^{-1}]
TCw	310 to 350	1.69	2000	923
PTn	250 to 310	0.85	1640	1360
TSw	-70 to 250	2.10	2200	930
CHnv	-155 to -70	0.84	2100	1220
CHnz	-250 to -155	1.42	1890	1420
CHnz (Sat)	-250 to -1000	1.56	2070	1230
Floor	n/a	0.60	2000	765
Backfill	n/a	fcn(T)	1200	765
Waste Package	n/a	50.00	7800	450

TCw = Tiva Canyon welded
PTn = Paintbrush nonwelded
TSw = Topopah Spring welded
CHnv = Calico Hills nonwelded vitric
CHnz = Calico Hills nonwelded zeolitic

Table 3. Effective Thermal Conductivity of Drift

Temperature [°C]	Before Backfilling [W m^{-1} K^{-1}]	After Backfilling [W m^{-1} K^{-1}]
20	5.0	0.20
70	7.6	0.23
120	11.1	0.28
170	15.6	0.34
220	21.2	0.41
270	28.0	0.49
320	36.1	0.59
370	45.9	0.70
420	57.0	0.84
470	70.0	0.99
520	84.9	1.15